# ACCOUNTS
of chemical research

Article

The O$_2$-Evolving Complex of Photosystem II: Recent Insights from Quantum Mechanics/Molecular Mechanics (QM/MM), Extended X-ray Absorption Fine Structure (EXAFS), and Femtosecond X-ray Crystallography Data

Mikhail Askerka, Gary W. Brudvig, and Victor S. Batista*

Department of Chemistry, Yale University, New Haven, Connecticut 06520-8107, United States

CONSPECTUS: Efficient photoelectrochemical water oxidation may open a way to produce energy from renewable solar power. In biology, generation of fuel due to water oxidation happens efficiently on an immense scale during the light reactions of photosynthesis. To oxidize water, photosynthetic organisms have evolved a highly conserved protein complex, Photosystem II. Within that complex, water oxidation happens at the CaMn$_4$O$_5$ inorganic catalytic cluster, the so-called oxygen-evolving complex (OEC), which cycles through storage "S" states as it accumulates oxidizing equivalents and produces molecular oxygen. In recent years, there has been significant progress in understanding the OEC as it evolves through the catalytic cycle. Studies have combined conventional and femtosecond X-ray crystallography with extended X-ray absorption fine structure (EXAFS) and quantum mechanics/molecular mechanics (QM/MM) methods and have addressed changes in protonation states of μ-oxo bridges and the coordination of substrate water through the analysis of ammonia binding as a chemical analog of water. These advances are thought to be critical to understanding the catalytic cycle since protonation states regulate the relative stability of different redox states and the geometry of the OEC. Therefore, establishing the mechanism for substrate water binding and the nature of protonation/redox state transitions in the OEC is essential for understanding the catalytic cycle of O$_2$ evolution.
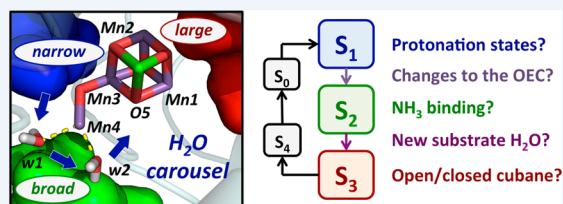
The structure of the dark-stable S$_1$ state has been a target for X-ray crystallography for the past 15 years. However, traditional X-ray crystallography has been hampered by radiation-induced reduction of the OEC. Very recently, a revolutionary X-ray free electron laser (XFEL) technique was applied to PSII to reveal atomic positions at 1.95 Å without radiation damage, which brought us closer than ever to establishing the ultimate structure of the OEC in the S$_1$ state. However, the atom positions in this crystal structure are still not consistent with high-resolution EXAFS spectroscopy, partially due to the poorly resolved oxygen positions next to Mn centers and partial reduction due to extended dark adaptation of the sample. These inconsistencies led to the new models of the OEC with an alternative low oxidation state and raised questions on the protonation state of the cluster, especially the O5 μ-oxo bridge. This Account summarizes the most recent models of the OEC that emerged from QM/MM, EXAFS and femtosecond X-ray crystallography methods.

When PSII in the S$_1$ state is exposed to light, the S$_1$ state is advanced to the higher oxidation states and eventually binds substrate water molecules. Identifying the substrate waters is of paramount importance for establishing the water-oxidation mechanism but is complicated by a large number of spectroscopically similar waters. Water analogues can, therefore, be helpful because they serve as spectroscopic markers that help to track the motion of the substrate waters. Due to a close structural and electronic similarity to water, ammonia has been of particular interest. We review three competing hypotheses on substrate water/ammonia binding and compile theoretical and experimental evidence to support them. Binding of ammonia as a sixth ligand to Mn4 during the S$_1 \rightarrow$ S$_2$ transition seems to satisfy most of the criteria, especially the most compelling recent EPR data on D1-D61A mutated PSII. Such a binding mode suggests delivery of water from the "narrow" channel through a "carousel" rearrangement of waters around Mn4 upon the S$_2 \rightarrow$ S$_3$ transition. An alternative hypothesis suggests water delivery through the "large" channel on the Ca side. However, both water delivery paths lead to a similar S$_3$ structure, seemingly reaching consensus on the nature of the last detectable S-state intermediate in the Kok cycle before O$_2$ evolution.

1. INTRODUCTION

Photosystem II (PSII) is a 350 kDa protein−pigment complex found in higher plants, algae, and cyanobacteria that has generated most of the atmospheric oxygen (O$_2$) during the light reactions of photosynthesis.[1,2] In PSII, upon light absorption, the primary chlorophyll-*a* species transfers an electron to pheophytin, forming the chlorophyll cation radical

P$_{680}^{\bullet+}$, which oxidizes the redox-active tyrosine Y$_Z$ next to the oxygen-evolving complex (OEC). The oxidized tyrosine in turn oxidizes the OEC, which is ultimately responsible for oxidation

of substrate water molecules, evolving O_2 and releasing protons to the lumen.

The OEC is a cuboidal Mn_4CaO_5 cluster (see Figure 1 for structure and atom numbering) composed of earth-abundant
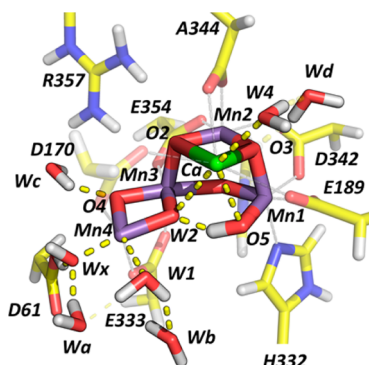

Figure 1. OEC and directly ligated residues, as well as second sphere residues D1-D61, D1-His337, and CP43-R357 and water molecules in the vicinity. Reproduced with permission from ref 3. Copyright 2016 American Chemical Society.

metal centers (i.e., Mn and Ca), linked by μ-oxo bridges (i.e., deprotonated water molecules) and ligated by side chains and termini of surrounding amino acid residues. Light absorption leads to cumulative oxidation of the OEC as it evolves through the so-called "storage states" S_0-S_4,[4,5] with S_1 being the dark-adapted resting state. After three flashes of light, it forms the S_4 state leading to O_2 evolution and regeneration of the S_0 state by water oxidation. Typical turnover frequencies showing oxidation of 100 H_2O molecules per second[6] under low overpotentials (70 mV)[7] make the OEC cluster a prototype model system for design of artificial water-oxidation catalysts. Therefore, understanding the nature of the OEC and its functionality during water oxidation remains a subject of great research interest.

2. STRUCTURE OF THE OEC IN THE DARK-ADAPTED S_1 STATE

2.1. Uncertainty in the 1.95 Å XFEL Structure

X-ray diffraction (XRD) has been instrumental in determining the structure of the OEC,[8−13] revealing the atomic coordinates of the OEC as well as the ligation scheme of surrounding residues and water molecules,[12] with increasing resolution from 3.8 to 1.9 Å over the past decade. However, models based on traditional XRD were affected by radiation damage. The relatively long exposure to a high dose of X-rays during data collection typically leads to Mn reduction and elongation of Mn−Mn distances, as suggested by extended X-ray absorption fine structure (EXAFS) and X-ray absorption near edge structure (XANES) spectroscopy[14,15] and quantum mechanics/molecular mechanics (QM/MM) hybrid methods.[16,17]

Recent advances in femtosecond X-ray crystallography using X-ray free electron laser (XFEL) facilities have addressed the challenge of radiation damage and have produced a PSII crystal model at 1.95 Å resolution with Mn−Mn distances notably shorter than those of the 2011 1.9 Å XRD structure. This new technology involves scattering of ultrashort (fwhm = 50 fs) X-ray pulses of an extremely high intensity, allowing for data collection on the femtosecond time scale before processes responsible for radiation damage can modify the sample.[18]

Despite these significant breakthroughs, consensus on the model of the OEC in the various S states has yet to be reached, partially due to limitations in the preparation of the system in a well-defined redox state (i.e., structural disorder) and partially due to ambiguities in the interpretation of the experimental data, even in the dark-stable S_1 state.

Several studies have focused on the protonation state of the O5 μ-oxo bridge in the S_1 state. A DFT analysis of the 1.95 Å XFEL model structure concluded the O5 μ-oxo bridge of the OEC was most likely protonated.[19] Within the "low" oxidation state paradigm,[20] the 1.95 Å XFEL structure was found to be most consistent with the oxidation state pattern of III, IV, III, and II for Mn1−Mn4, respectively, with W2 being a terminal H_2O ligand and O5 being a OH ligand bridging Ca and Mn centers.[20] A comprehensive comparison of the "high" and "low" oxidation state paradigms has shown that the "low" oxidation is much less supported by experiments.[21] Our analysis of the PDB structures 4UB6 and 4UB8 suggests that X-ray scattering leaves more uncertainty in the positions of O atoms than for heavier Mn and Ca centers.[22] The origin of the uncertainty is the significantly lower intensity of X-ray scattering from μ-oxo bridges, often overshadowed by strong scattering from adjacent Mn centers with as much as three times larger electronic density (Figure 2A). In addition, resolving the positions of lighter atoms next to the heavier atoms is usually complicated due to the Fourier truncation ripple effect.[22] For the OEC, the position of the first Fourier ripple from Mn coincides approximately with the position of the O in the μ-oxo bridge, therefore introducing additional uncertainty on the actual position of the O center (Figure 2, B).

Uncertainty in the position of the O atoms leads to disagreement between the experimental EXAFS spectra and simulations based on the coordinates from the 4UB6 and 4UB8 structures, as shown by direct comparisons with the experimental S_1 extended range EXAFS spectrum (Figure 2C).[23] In addition, the comparison suggests the possibility of structural disorder (mixture of S states in the crystallized PSII samples) with a significant fraction of the OEC cores poised in the S_0 state, rather than purely S_1, due to extensive (1 week) dark adaptation.

There may be an additional reason for the structural disorder in the 1.95 Å XFEL structure.[18] In that experiment, the diffraction data were collected using XFEL pulses that were shot at equally spaced points (50 μm) on the same crystal. It has been very recently shown that the hydroxyl radicals originating from the XFEL pulses can travel long distances within the crystal and their diffusion rate is higher than the speed of sample translation.[24] The diffraction data in the 1.95 Å XFEL structure may have been, therefore, collected on a partially damaged crystal.

2.2. Protonation States of the Water Ligands in the OEC

While the pattern of the proton release in the Kok cycle is well established, the protonation state of the OEC in the dark-stable S_1 state is still a matter of debate. Despite the tremendous amount of computational work on various mechanistic aspects of the OEC, a consensus on the protonation states has not yet been reached even for the models reported within past two years (Table 1).

The QM/MM (or QM) + EXAFS-based models[22,25] (Table 1, entry 1) suggest having a doubly protonated (positively charged) His337, H_2O as the W2 ligand, and nonprotonated O5. Using QM/MM and QM models, Yamaguchi and co-
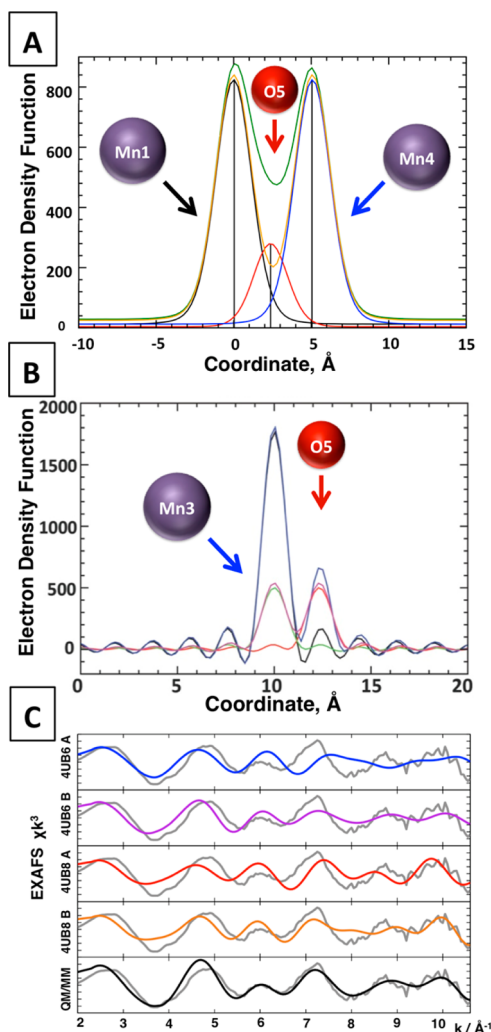
Figure 2. (A) Simulated electron density profile of the Mn1−O5−Mn4 coordinate shows that the O positions are overshadowed by a strong Mn signal. (B) Simulated electron density profile of Mn3−O5 shows that the O positions approximately coincide with the first Fourier ripple from Mn. (C) EXAFS spectra simulated from different monomers and data sets of the 1.95 Å XFEL structure[18] compared to the experimental[14] S_1 spectrum (gray) and QM/MM model[17] (black). Adapted with permission from the main text the SI of ref 22. Copyright 2015 American Chemical Society.

workers[19] (Table 1, entry 2) proposed that the best agreement with the 1.95 Å XFEL structure is achieved when the proton from W2 is relocated to O5, while keeping the His337 residue neutral. The protonation state of O5 was studied extensively by Knapp[26] (Table 1, entry 3) using QM models. In that study, depending on the protonation state on W2 and His337, the pK_a of O5 varied from −0.8 to 4.7 when using a dielectric constant $\varepsilon = 20$ and from 1.2 to 7.4 for $\varepsilon = 80$. Because $\varepsilon = 80$, which corresponds to the dielectric constant of water, is an extreme upper bound for the dielectric constant in a protein, it would be safe to assume that O5 remains unprotonated in S_1 state. Based on EPR/ENDOR studies, it was concluded that one of the Mn4 ligands,[31] most likely W2 is deprotonated (Table 1, entry 4). This result carried on to several models currently used in the literature.[27−29] Expectedly, the low oxidation state paradigm models[20] predict maximum hydration (H_2O at W2, OH at O5, and doubly protonated His337) for the S_1 state (Table 1, entry 5).

Table 1. Comparison of the Protonation States in the S_1 OEC Models Suggested by Experiments and Theory

		protonation states		
	S_1 state	W2	O5	His337
1	Batista (2015),[22] Yano (2016)[25,a]	H_2O	O	$N_\delta H$, $N_\varepsilon H$
2	Yamaguchi (2015)[19]	OH^-	OH^-	$N_\varepsilon H$
3	Knapp (2014),[26] Siegbahn (2014)[27]	OH^-	O	$N_\varepsilon H$
4	Neese (2012),[28] Kaila (2016),[29,a] Siegbahn (2014)[27]	OH^-	O	$N_\delta H$, $N_\varepsilon H$
5	Pace (2015)[20,b]	H_2O	OH^-	$N_\delta H$, $N_\varepsilon H$

[a]The S_1 state is deduced from the structure of the S_2 state given that the S_1 to S_2 transition does not involve a proton relocation. [b]The "low" oxidation states paradigm (III, IV, III, II). Guidoni[30] employs the coordinates from Neese.[28] Structures 2 and 5 are essentially the S_1 crystal structure without (QM or EXAFS) refinement.

DFT models of the OEC suggest that barriers for O−O bond formation could be similar for single ($N_\varepsilon H$) and double ($N_\delta H$, $N_\varepsilon H$) protonation states of His337,[27] although the potential for oxidation of the OEC compared to the Tyr_z−His190 pair is higher with double protonation. The pK_a's of the OEC are also modulated by different protonation states,[26] that also modulate magnetic couplings.[31]

3. S_2 STATE

3.1. $S_1 \rightarrow S_2$ Transition

The $S_1 \rightarrow S_2$ transition is the only transformation of the OEC that does not involve proton transfer to the lumen and is observed even at cryogenic temperatures.[32,33] The resulting structural changes to the OEC are thus solely due to the oxidation process and are, therefore, small and difficult to probe. Traditionally, most of the analysis of the $S_1 \rightarrow S_2$ oxidation state transition has been based on EPR,[34,35] EXAFS,[36] time-resolved mass spectroscopy,[37,38] and FTIR.[32,39−41] Recently, the femtosecond XFEL technique has been applied to microcrystals of the OEC in the S_1 and S_2 states; however, no significant changes in the structure of the OEC could be detected upon $S_1 \rightarrow S_2$ transition due to the limited resolution of the diffraction data (5.9 Å).[42] A subsequent study based on the isomorphous Fourier difference method, however, revealed a clear change in the electron density maps around Mn4 induced by the $S_1 \rightarrow S_2$ transition (Figure 3).[43] The change was due to a slight displacement of Mn4 toward the body of the cubane and a change of its coordination environment toward a more symmetric octahedron, as expected for a $Mn^{3+} \rightarrow Mn^{4+}$ transition. The underlying oxidation state transition and structural rearrangements were found to be consistent with the simulating electron density difference obtained from QM/MM models as calculated at comparable (5.9 Å) resolution (Figure 3)[43] but do not support the proton relocation (O5 → W2) that is widely proposed to accompany manganese oxidation.[19]

3.2. Ammonia Binding to the S_2 state

Studies of ammonia binding to PSII have been focused on the S_1 and S_2 states. Ammonia binding provides mechanistic
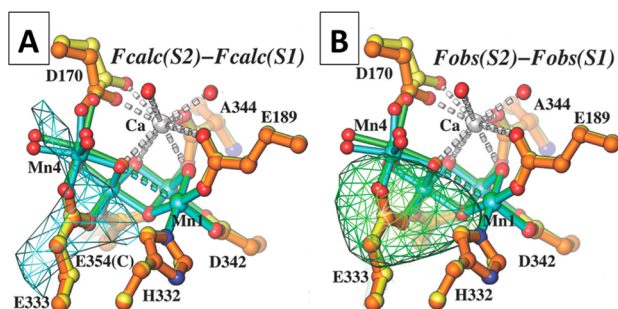
Figure 3. QM/MM S_1 and S_2 models and difference Fourier maps. (A) Simulated S_2-minus-S_1 difference Fourier maps calculated using the QM/MM S_1 and S_2 models and phases derived from multicrystal noncrystallographic symmetry averaging. (B) Observed S_2-minus-S_1 difference Fourier maps calculated from ref 42. The highest peak near the OEC results from the displacement of Mn4, which can be explained through Mn4^{3+} → Mn4^{4+} oxidation upon the S_1 → S_2 transition. Adapted with permission from ref 43. Copyright 2014 American Chemical Society.

insights because ammonia is a structural and electronic analog of water. Therefore, ammonia serves as a marker to probe the potential binding mode and exchange of water.

Two different ammonia-binding sites have been analyzed by experiments and QM/MM modeling.[44] A so-called "secondary" site was proposed in the vicinity of the OEC, leaving ammonia in the second coordination sphere without any direct contact with the OEC cluster.[45,46] Binding to that site is competitive with Cl$^-$ binding and happens in the S_1 state.[46,47]

The "primary" ammonia-binding site most likely involves coordination to Mn4 induced by the S_1 → S_2 transition and is not competitive with Cl$^-$ binding. Remarkably, ammonia binding to the "primary" site does not block the catalytic turnover.[48,49] Currently, there are three competing hypotheses (Table 2) regarding the ammonia specific binding modes: (i) ammonia binds, replaces O5, and binds in a bridging motif; (ii) ammonia binds to Mn4 as a terminal ligand by exchange with

W1; (iii) ammonia binds as an additional sixth terminal ligand to Mn4.

The analysis of ^{14}NH$_4$Cl and ^{15}NH$_4$Cl treated PSII samples, based on early electron spin echo envelope modulation (ESEEM) experiments,[52] showed nuclear quadrupole couplings that could be interpreted by comparison with model compounds in terms of an NH$_2$ bridge between two Mn centers.[52] The FTIR difference experiments showed a loss of a Mn−O−Mn bending signal upon ammonia binding, at about 601 cm^{-1}, which was indicative of the loss of one μ-oxo bridge. The analysis was in line with hypotheses a and c but could not be explained by hypothesis b. Ammonia binding also changes the geometry of the OEC cubane, most likely elongating one of the Mn−Mn distances, as evidenced by EXAFS.[51] The combination of QM/MM models and EXAFS simulations has shown that such changes can be introduced by either replacing a μ-oxo bridge (a) or by adding ammonia as a sixth ligand to Mn4 (b). Replacing a terminal water by ammonia has been disfavored since such a ligand exchange leaves the geometry of the cluster almost unaltered.[56] This is in contrast to the substantial structural changes of the OEC suggested by the recent S_2 → S_1 decay experiments[35] that predicted a significant decrease in the S_2 reduction potential (120 mV) induced by ammonia binding.

The primary binding site is accessible for ammonia but not for larger amines,[46] which could be consistent with the bridging binding motif (b) when such a coordination mode is disfavored for larger ligands. However, it could also be consistent with binding as a terminal ligand (b, c) when binding involves deprotonation, a process that is more difficult for larger protonated amines, with higher pK$_a$.[56]

The DFT analysis of ammonia binding has disfavored the bridging binding motif (a), predicting much higher binding energies (>20 kcal/mol) for ammonia replacing W1.[53] The ^{17}O-EDNMR spectral envelopes[54] of ammonia bound PSII were also interpreted in terms of ammonia replacing W1, perturbing O5 via a *trans*-effect. Recently, compelling evidence of ammonia hydrogen bonded to D61 was offered by EPR experiments on native and D61A mutated PSII,[55] therefore supporting binding as a terminal ligand (b or c).

Ammonia binding to the primary site, as an additional ligand of Mn4, is consistent with migration from the secondary site, upon S_1 → S_2 oxidation of the OEC.[57] Such a binding process could be common to substrate water binding, although later in the cycle since ammonia is a "harder" Lewis base than water.[56] Therefore, it has been proposed that substrate water binds to the primary ammonia-binding site during the S_2 → S_3 state transition, upon migration from the secondary site.

4. S_2 → S_3 TRANSITION

4.1. Open and Closed Forms of the OEC in the S_3 State

EPR experiments have established the existence of two spin isomers of the OEC in the S_2 state, which give rise to the g = 2.0 multiline signal from a spin 1/2 state[58] and the g = 4.1 signal from a spin 5/2 state.[59,60] QM/MM[61] and DFT[28] suggested models where the position of O5 is closer to Mn1 in the g = 4.1 "closed" isomer or closer to Mn4 in the g = 2.0 open isomer.

Recently, both "closed" and "open" conformers were proposed for the S_3 state with all Mn centers in the oxidation state IV.[62,63] The "open" S_3, however, has been shown to be significantly more stable[3,29,62] and is likely representative of the

Table 2. Comparison of Ammonia-Bound OEC Models Suggested by Experiments and Theory

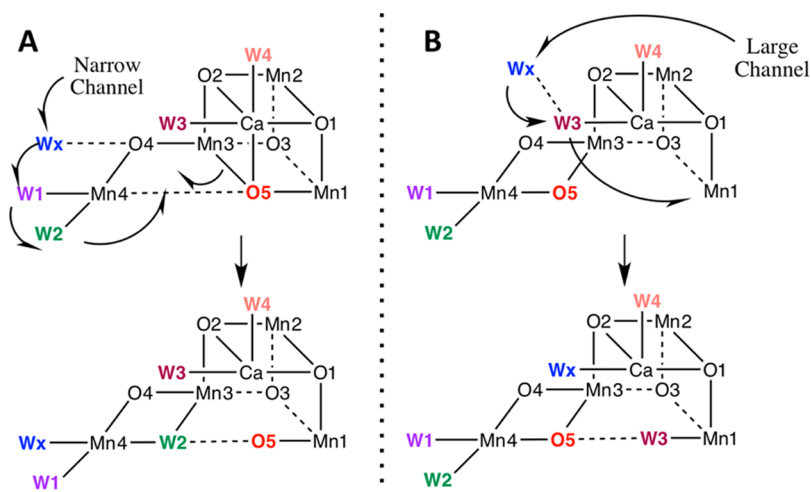|		binding site		
	experiment	(a) bridging: replacing O5	(b) terminal: replacing W1	(c) terminal: 6th ligand to Mn4
1	FTIR: loss of the Mn-O-Mn band at 601 cm^{-1}[50]	yes	no	yes
2	EXAFS: one Mn-Mn gets longer[51] (x2)	yes	no	yes
3	S2 reduction potential decrease (120 mV)[35]	yes	no	yes
4	ESEEM[52]	yes	yes	yes
5	larger amines do not bind[46]	yes	in part	in part
6	DFT energetics[53]	no	yes	yes
7	^{17}O-EDNMR W-band[54]	no	yes	in part
8	EPR on D-61A mutant[55] (x2)	no	yes	yes

Figure 4. Two hypotheses on the origin and pathway for binding of a water molecule during the $S_2 \rightarrow S_3$ transition, leading to a qualitatively similar S_3 state. (A) Wx is the water initially hydrogen bonded to O4; upon oxidation, it triggers a carousel/pivot rearrangement of the waters around Mn4. (B) Wx is initially bonded to W3; the rearrangement happens on the Ca side of the OEC.

experimental S_3 EXAFS spectrum.[3] A recent study that combined the QM/MM models with an analysis of the difference Fourier density maps from XFEL data on PSII microcrystals[64] showed that the $S_1 \rightarrow S_3$ transition involves expansion of the cubane.[3] The resulting expansion was surprising since oxidation of Mn(III) typically contracts coordination bond lengths upon loss of Jahn–Teller elongated bonds and, therefore, cannot be explained by domination of S_1 or S_2 in the microcrystals.[64] However, it is found that while the coordination bond lengths do become shorter, the "open" cubane structure is slightly expanded upon binding an additional water molecule to Mn4, which deprotonates to form a di-μ-oxo bridge between Mn3 and Mn4, leaving a protonated O5 ligand bound to Mn1, as shown in (Figure 4A or B, lower panel),[3] qualitatively similar to an S_3 model, that was proposed to form through binding of a water molecule to Mn1.[65]

4.2. Water Binding

There is currently significant consensus on the structure of the OEC in the S_3 state although the $S_2 \rightarrow S_3$ transition remains a subject of debate. The formation of the S_3 state likely involves binding of a water ligand,[3,66−68] along with oxidation of one of the Mn centers. However, there are currently two hypotheses on the origin and binding mode of the water molecule (Figure 4), including binding to the dangling Mn through a carousel/pivot mechanism (A) or binding to Mn1 according to pathway B.

While the narrow channel delivery pathway (A) is consistent with experiments, the alternative mechanism (B) has been proposed by a computational study,[29] suggesting water delivery through the "large channel" that starts from water molecules W3 and W4, ligated to Ca, and branches out to reach the interface on CP43 and PsbV or PsbV and PsbU subunits. Among the water molecules directly ligated to the OEC, W3 has been predicted to have the lowest proton affinity in the S_2 $Y_Z^\bullet$ state.[29] That has motivated the proposal that oxidation of an S_2 state that already has a di-μ-oxo bridge linking Mn3 and Mn4 might somehow lead to deprotonation of the Ca water ligand W3 and induce binding of OH ligand to Mn1. This mechanism is supported by the mutation experiments on the

Ca side of PSII[69] (V185N, hydrogen bonded to W3) that slows down the further advancement of S_3.

The OEC is surrounded by a water network that can be divided into three major channels: the so-called "narrow", "broad", and "large" channels (Figure 5).[70] According to
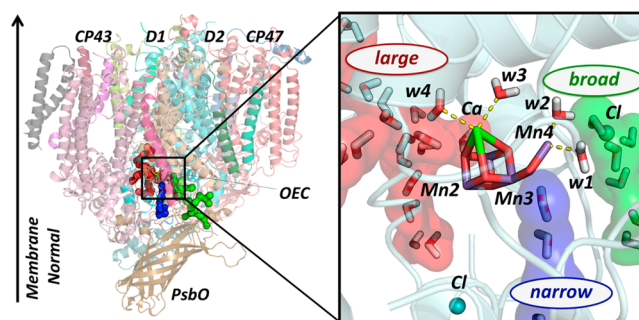

Figure 5. Water network channels in PSII as they are situated in the protein subunits (left) and surrounding OEC (right). Competing hypotheses propose either the narrow channel (blue) or the large channel (red) to be responsible for water delivery in the $S_2 \rightarrow S_3$ transition. Shown in sticks are the OEC and directly coordinated water molecules (w1−w4). The high-affinity chloride in the broad channel (green) and the low affinity chloride next to the narrow channel are shown in cyan. The atom positions are taken from the QM/MM S_2 g = 4.1 state model.[56]

pathway A, a water molecule (Wx) is delivered through the narrow "channel" and binds to Mn4 during the $S_2 \rightarrow S_3$ transition. In cyanobacteria, the "narrow" channel starts at the O4 μ-oxo bridge of the OEC and reaches the interface of the PsbO and PsbU subunits. Such a pathway is consistent with the analysis of ammonia binding and inhibition of PSII. As mentioned in section 3.2, ammonia likely binds to the "secondary" binding site, establishing a hydrogen-bond network bridging the carboxylate of D61 and the water ligand (W1) of the dangling Mn4. From the secondary site, which is embedded in the "narrow" channel, ammonia likely migrates and binds to Mn4. Since water and ammonia are structural and electronic analogs, it is reasonable to assume that water is also delivered by the narrow channel and binds to Mn4 during the $S_2 \rightarrow S_3$ transition.[3] Mechanistically, it is proposed that the $S_2 \rightarrow S_3$

transition advances the oxidation state of Mn4, triggering binding of water (Wx) to the dangling Mn, and inducing the rearrangement of other water molecules in a carousel around Mn4. An analogous "pivot" rearrangement that relies on the assignment of the near IR active portion of S_3 has been recently proposed computationally.[71] The barrier for displacement of Wx has been estimated to be around 8 kcal mol^{-1}, which is lower than the barrier for binding any other water molecule in the vicinity of Mn4.[72] Such a barrier thus lines up well with the estimated barrier (9 kcal/mol) for water *entry into* the "narrow" channel.[73]

Summarizing the water delivery pathways in the S_2 to S_3 transition, we note that the carousel/pivot mechanisms (Figure 4A) proposed by computational studies are supported by EXAFS studies of ammonia binding to the S_2 state and by near-infrared absorption studies and EPR spectroscopy. Water entry from the Ca side of the OEC (Figure 4B) has been indirectly supported by mutagenesis experiments. However, more experimental studies are necessary to support or otherwise rule out either of the two currently proposed water delivery pathways.

5. CONCLUDING REMARKS

We have reviewed recent advances on the characterization of the OEC in the various redox states along the catalytic cycle of O_2 evolution. Understanding changes in the protonation state of the OEC and the pathway for substrate water binding is essential for characterization of the catalytic mechanism of O−O bond formation and design of biomimetic systems. Recent studies combining the analysis of electron density maps obtained from femtosecond XFEL diffraction experiments in conjunction with QM/MM calculations, mutagenesis experiments, and high resolution EXAFS and IR spectroscopy have provided valuable insights into the structure and function of the OEC and the underlying transitions along the catalytic cycle, including changes in protonation/redox states and the mechanism of substrate water binding. We anticipate these techniques will continue to make significant contributions to the field.

■ AUTHOR INFORMATION

Corresponding Author

*E-mail: victor.batista@yale.edu. Phone: (203) 432-6672. Fax: (203) 432 6144.

ORCID

Gary W. Brudvig: 0000-0002-7040-1892

Notes

The authors declare no competing financial interest.

Biographies

Mikhail Askerka (1990, Moscow, Russia) received a M.S. (2011) in Chemistry from Moscow State University where he was working with Daria Pichugina and Nikolay Kuz'menko. After brief postgraduate research experince, he moved on to the Chemistry Department of Yale University to pursue a Ph.D. in Physical Chemistry with Victor Batista and John Tully. His research focuses on the computational studies of Photosystem II and development of new methodologies to describe electronic friction of molecules on metal surfaces.

Gary W. Brudvig (1954, Grand Forks, ND, USA) received a B.S. (1976) from the University of Minnesota and a Ph.D. (1981) from Caltech working with Sunney Chan and was a Miller Postdoctoral Fellow at the University of California, Berkeley, from 1980 to 1982 with Ken Sauer. He has been on the faculty at Yale since 1982, where he currently is the Benjamin Silliman Professor and Chair of Chemistry, Professor of Molecular Biophysics and Biochemistry, and Director of the Yale Energy Sciences Institute. His research involves study of the chemistry of solar energy conversion in photosynthesis and work to develop artificial bioinspired systems for solar fuel production.

Victor S. Batista (1966, Buenos Aires, Argentina) received his Lic. Ciencias Quimicas degree from Universidad de Buenos Aires, Argentina (1989), and the Sugata Ray Award (1995) and a Ph.D. degree in Theoretical Chemistry (1996) from Boston University. After completing postdoctoral programs with William H. Miller at the University of California, Berkeley (1997−1999), and Paul Brumer at the University of Toronto (2000), he joined the Yale faculty in 2001, where he has received the ACS PRF-G6 Award (2002), the Research Corporation Innovation Award (2002), the NSF Career Award (2004), the Sloan Fellowship (2005−2006), and the Camille Dreyfus Teacher-Scholar Award (2005).

■ REFERENCES

(1) McEvoy, J. P.; Brudvig, G. W. Water-Splitting Chemistry of Photosystem II. *Chem. Rev.* **2006**, *106*, 4455−4483.

(2) Nelson, N.; Yocum, C. F. Structure and Function of Photosystems I and II. *Annu. Rev. Plant Biol.* **2006**, *57*, 521−565.

(3) Askerka, M.; Wang, J.; Vinyard, D. J.; Brudvig, G. W.; Batista, V. S. S_3 State of the O_2-Evolving Complex of Photosystem II: Insights from QM/MM, EXAFS, and Femtosecond X-ray Diffraction. *Biochemistry* **2016**, *55*, 981−984.

(4) Joliot, P.; Kok, B. Oxygen Evolution in Photosynthesis. In *Bioenergetics of Photosynthesis*; Govindjee, Ed.; Academic Press: New York, 1975; pp 387−412.

(5) Kok, B.; Forbush, B.; Mcgloin, M. Cooperation of Charges in Photosynthetic O_2 Evolution-I. A Linear Four Step Mechanism. *Photochem. Photobiol.* **1970**, *11*, 457−475.

(6) Blankenship, R. E. Frontmatter. In *Molecular Mechanisms of Photosynthesis*; Blackwell Science Ltd.: Oxford, U.K., 2008; pp i−vii.

(7) Grabolle, M.; Dau, H. Energetics of Primary and Secondary Electron Transfer in Photosystem II Membrane Particles of Spinach Revisited on Basis of Recombination-Fluorescence Measurements. *Biochim. Biophys. Acta, Bioenerg.* **2005**, *1708*, 209−218.

(8) Ferreira, K. N.; Iverson, T. M.; Maghlaoui, K.; Barber, J.; Iwata, S. Architecture of the Photosynthetic Oxygen-Evolving Center. *Science* **2004**, *303*, 1831−1838.

(9) Guskov, A.; Kern, J.; Gabdulkhakov, A.; Broser, M.; Zouni, A.; Saenger, W. Cyanobacterial Photosystem II at 2.9-Å Resolution and the Role of Quinones, Lipids, Channels and Chloride. *Nat. Struct. Mol. Biol.* **2009**, *16*, 334−342.

(10) Kamiya, N.; Shen, J. R. Crystal Structure of Oxygen-Evolving Photosystem II from *Thermosynechococcus Vulcanus* at 3.7-Å Resolution. *Proc. Natl. Acad. Sci. U. S. A.* **2003**, *100*, 98−103.

(11) Loll, B.; Kern, J.; Saenger, W.; Zouni, A.; Biesiadka, J. Towards Complete Cofactor Arrangement in the 3.0 Angstrom Resolution Structure of Photosystem II. *Nature* **2005**, *438*, 1040−1044.

(12) Umena, Y.; Kawakami, K.; Shen, J.-R.; Kamiya, N. Crystal Structure of Oxygen-evolving Photosystem II at a Resolution of 1.9 angstrom. *Nature* **2011**, *473*, 55−60.

(13) Zouni, A.; Witt, H. T.; Kern, J.; Fromme, P.; Krauß, N.; Saenger, W.; Orth, P. Crystal Structure of Photosystem II from *Synechococcus elongatus* at 3.8 Å Resolution. *Nature* **2001**, *409*, 739−743.

(14) Grundmeier, A.; Dau, H. Structural Models of the Manganese Complex of Photosystem II and Mechanistic Implications. *Biochim. Biophys. Acta, Bioenerg.* **2012**, *1817*, 88−105.

(15) Yano, J.; Kern, J.; Irrgang, K. D.; Latimer, M. J.; Bergmann, U.; Glatzel, P.; Pushkar, Y.; Biesiadka, J.; Loll, B.; Sauer, K.; Messinger, J.; Zouni, A.; Yachandra, V. K. X-Ray Damage to the Mn_4Ca Complex in Single Crystals of Photosystem II: A Case Study for Metalloprotein Crystallography. *Proc. Natl. Acad. Sci. U. S. A.* **2005**, *102*, 12047−12052.

(16) Luber, S.; Rivalta, I.; Umena, Y.; Kawakami, K.; Shen, J.-R.; Kamiya, N.; Brudvig, G. W.; Batista, V. S. S_1-state Model of the O_2-Evolving Complex of Photosystem II. *Biochemistry* **2011**, *50*, 6308−6311.

(17) Pal, R.; Negre, C. F. A.; Vogt, L.; Pokhrel, R.; Ertem, M. Z.; Brudvig, G. W.; Batista, V. S. S_0-state Model of the Oxygen-Evolving Complex of Photosystem II. *Biochemistry* **2013**, *52*, 7703−7706.

(18) Suga, M.; Akita, F.; Hirata, K.; Ueno, G.; Murakami, H.; Nakajima, Y.; Shimizu, T.; Yamashita, K.; Yamamoto, M.; Ago, H.; Shen, J.-R. Native Structure of Photosystem II at 1.95 A Resolution Viewed by Femtosecond X-Ray Pulses. *Nature* **2014**, *517*, 99−103.

(19) Shoji, M.; Isobe, H.; Yamanaka, S.; Suga, M.; Akita, F.; Shen, J. R.; Yamaguchi, K. Theoretical Studies of the Damage-free S_1 Structure of the $CaMn_4O_5$ Cluster in Oxygen-Evolving Complex of Photosystem II. *Chem. Phys. Lett.* **2015**, *623*, 1−7.

(20) Petrie, S.; Pace, R. J.; Stranger, R. Resolving the Differences Between the 1.9 and 1.95 A Crystal Structures of Photosystem II: A Single Proton Relocation Defines Two Tautomeric Forms of the Water-Oxidizing Complex. *Angew. Chem., Int. Ed.* **2015**, *54*, 7120−7124.

(21) Krewald, V.; Neese, F.; Pantazis, D. A. Resolving the Manganese Oxidation States in the Oxygen-evolving Catalyst of Natural Photosynthesis. *Isr. J. Chem.* **2015**, *55*, 1219−1232.

(22) Askerka, M.; Vinyard, D. J.; Wang, J. M.; Brudvig, G. W.; Batista, V. S. Analysis of the Radiation-Damage-Free X-ray Structure of Photosystem II in Light of EXAFS and QM/MM Data. *Biochemistry* **2015**, *54*, 1713−1716.

(23) Dau, H.; Grundmeier, A.; Loja, P.; Haumann, M. On the Structure of the Manganese Complex of Photosystem II: Extended-Range EXAFS Data and Specific Atomic-Resolution Models for Four S-States. *Philos. Trans. R. Soc., B* **2008**, *363*, 1237−1243.

(24) Wang, J. Oxygen Additions in Serial Femtosecond Crystallographic Protein Structures. *Protein Sci.* **2016**, *25*, 1797−1802.

(25) Chatterjee, R.; Han, G.; Kern, J.; Gul, S.; Fuller, F. D.; Garachtchenko, A.; Young, I. D.; Weng, T.-C.; Nordlund, D.; Alonso-Mori, R.; Bergmann, U.; Sokaras, D.; Hatakeyama, M.; Yachandra, V. K.; Yano, J. Structural Changes Correlated with Magnetic Spin State Isomorphism in the S_2 State of the Mn_4CaO_5 Cluster in the Oxygen-Evolving Complex of Photosystem II. *Chem. Sci.* **2016**, *7*, 5236.

(26) Galstyan, A.; Robertazzi, A.; Knapp, E. W. Oxygen-Evolving Mn Cluster in Photosystem II: The Protonation Pattern and Oxidation State in the High-Resolution Crystal Structure. *J. Am. Chem. Soc.* **2012**, *134*, 7442−7449.

(27) Siegbahn, P. E. M. Water Oxidation Energy Diagrams for Photosystem II for Different Protonation States, and the Effect of Removing Calcium. *Phys. Chem. Chem. Phys.* **2014**, *16*, 11893−11900.

(28) Pantazis, D. A.; Ames, W.; Cox, N.; Lubitz, W.; Neese, F. Two Interconvertible Structures that Explain the Spectroscopic Properties of the Oxygen-Evolving Complex of Photosystem II in the S_2 State. *Angew. Chem., Int. Ed.* **2012**, *51*, 9935−9940.

(29) Ugur, I.; Rutherford, A. W.; Kaila, V. R. Redox-Coupled Substrate Water Reorganization in the Active Site of Photosystem II − the Role of Calcium in Substrate Water Delivery. *Biochim. Biophys. Acta, Bioenerg.* **2016**, *1857*, 740−748.

(30) Bovi, D.; Narzi, D.; Guidoni, L. The S_2 State of the Oxygen-Evolving Complex of Photosystem II Explored by QM/MM Dynamics: Spin Surfaces and Metastable States Suggest a Reaction Path Towards the S_3 State. *Angew. Chem., Int. Ed.* **2013**, *52*, 11744−11749.

(31) Ames, W.; Pantazis, D. A.; Krewald, V.; Cox, N.; Messinger, J.; Lubitz, W.; Neese, F. Theoretical Evaluation of Structural Models of the S_2 State in the Oxygen Evolving Complex of Photosystem II: Protonation States and Magnetic Interactions. *J. Am. Chem. Soc.* **2011**, *133*, 19743−19757.

(32) Iizasa, M.; Suzuki, H.; Noguchi, T. Orientations of Carboxylate Groups Coupled to the Mn Cluster in the Photosynthetic Oxygen-Evolving Center As Studied by Polarized ATR-FTIR Spectroscopy. *Biochemistry* **2010**, *49*, 3074−3082.

(33) de Paula, J. C.; Innes, J. B.; Brudvig, G. W. Electron Transfer in Photosystem II at Cryogenic Temperatures. *Biochemistry* **1985**, *24*, 8114−8120.

(34) Miller, A. F.; Brudvig, G. W. A Guide to Electron-Paramagnetic Resonance Spectroscopy of Photosystem-II Membranes. *Biochim. Biophys. Acta, Bioenerg.* **1991**, *1056*, 1−18.

(35) Vinyard, D. J.; Brudvig, G. W. Insights into Substrate Binding to the Oxygen-Evolving Complex of Photosystem II from Ammonia Inhibition Studies. *Biochemistry* **2015**, *54* (2), 622−628.

(36) Haumann, M.; Muller, C.; Liebisch, P.; Iuzzolino, L.; Dittmer, J.; Grabolle, M.; Neisius, T.; Meyer-Klaucke, W.; Dau, H. Structural and Oxidation State Changes of the Photosystem II Manganese Complex in Four Transitions of the Water Oxidation Cycle ($S_0 \rightarrow S_1$, $S_1 \rightarrow S_2$, $S_2 \rightarrow S_3$, and $S_4 \rightarrow S_0$) Characterized by X-ray Absorption Spectroscopy at 20 K and Room Temperature. *Biochemistry* **2005**, *44*, 1894−1908.

(37) Messinger, J.; Badger, M.; Wydrzynski, T. Detection of One Slowly Exchanging Substrate Water Molecule in the S_3 State of Photosystem-II. *Proc. Natl. Acad. Sci. U. S. A.* **1995**, *92*, 3209−3213.

(38) Hillier, W.; Wydrzynski, T. Substrate Eater Interactions within the Photosystem II Oxygen Evolving Complex. *Phys. Chem. Chem. Phys.* **2004**, *6*, 4882−4889.

(39) Debus, R. J. The Manganese and Calcium-Ions of Photosynthetic Oxygen Evolution. *Biochim. Biophys. Acta, Bioenerg.* **1992**, *1102*, 269−352.

(40) Debus, R. J. Protein Ligation of the Photosynthetic Oxygen-Evolving Center. *Coord. Chem. Rev.* **2008**, *252*, 244−258.

(41) Chu, H. A.; Hillier, W.; Debus, R. J. Evidence that the C-terminus of the D1 Polypeptide of Photosystem II is Ligated to the Manganese Ion that Undergoes Oxidation During the S_1 to S_2 Transition: An Isotope-Edited FTIR study. *Biochemistry* **2004**, *43*, 3152−3166.

(42) Kern, J.; Alonso-Mori, R.; Tran, R.; Hattne, J.; Gildea, R. J.; Echols, N.; Glockner, C.; Hellmich, J.; Laksmono, H.; Sierra, R. G.; Lassalle-Kaiser, B.; Koroidov, S.; Lampe, A.; Han, G.; Gul, S.; Difiore, D.; Milathianaki, D.; Fry, A. R.; Miahnahri, A.; Schafer, D. W.; Messerschmidt, M.; Seibert, M. M.; Koglin, J. E.; Sokaras, D.; Weng, T. C.; Sellberg, J.; Latimer, M. J.; Grosse-Kunstleve, R. W.; Zwart, P. H.; White, W. E.; Glatzel, P.; Adams, P. D.; Bogan, M. J.; Williams, G. J.; Boutet, S.; Messinger, J.; Zouni, A.; Sauter, N. K.; Yachandra, V. K.; Bergmann, U.; Yano, J. Simultaneous Femtosecond X-Ray Spectroscopy and Diffraction of Photosystem II at Room Temperature. *Science* **2013**, *340*, 491−495.

(43) Askerka, M.; Wang, J.; Brudvig, G. W.; Batista, V. S. Structural Changes in the Oxygen-Evolving Complex of Photosystem II Induced by the S_1 to S_2 Transition: A Combined XRD and QM/MM Study. *Biochemistry* **2014**, *53*, 6860−6862.

(44) Sandusky, P. O.; Yocum, C. F. The Chloride Requirement for Photosynthetic Oxygen Evolution: Analysis of the Effects of Chloride

and Other Anions on Amine Inhibition of the Oxygen-Evolving Complex. *Biochim. Biophys. Acta, Bioenerg.* **1984**, *766*, 603−611.

(45) Sandusky, P. O.; Yocum, C. F. The Chloride Requirement for Photosynthetic Oxygen Evolution: Factors Affecting Nucleophilic Displacement of Chloride from the Oxygen-Evolving Complex. *Biochim. Biophys. Acta, Bioenerg.* **1986**, *849*, 85−93.

(46) Beck, W. F.; Brudvig, G. W. Binding of Amines to the Oxygen-Evolving Center of Photosystem II. *Biochemistry* **1986**, *25*, 6479−6486.

(47) Sandusky, P.; Yocum, C. The Relationship Between the Chloride Requirement of Oxygen Evolution and Amine Inhibition. *Plant Physiol* **1984**, *75*, 113−113.

(48) Beck, W. F.; de Paula, J. C.; Brudvig, G. W. Ammonia Binds to the Manganese Site of the Oxygen-Evolving Complex of Photosystem II in the S_2 state. *J. Am. Chem. Soc.* **1986**, *108*, 4018−4022.

(49) Boussac, A.; Rutherford, A. W.; Styring, S. Interaction of Ammonia with the Water Splitting Enzyme of Photosystem-II. *Biochemistry* **1990**, *29*, 24−32.

(50) Hou, L.-H.; Wu, C.-M.; Huang, H.-H.; Chu, H.-A. Effects of Ammonia on the Structure of the Oxygen-Evolving Complex in Photosystem II as Revealed by Light-Induced FTIR Difference Spectroscopy. *Biochemistry* **2011**, *50*, 9248−9254.

(51) Dau, H.; Andrews, J. C.; Roelofs, T. A.; Latimer, M. J.; Liang, W. C.; Yachandra, V. K.; Sauer, K.; Klein, M. P. Structural Consequences of Ammonia Binding to the Manganese Center of the Photosynthetic Oxygen-Evolving Complex - an X-Ray-Absorption Spectroscopy Study of Isotropic and Oriented Photosystem-II Particles. *Biochemistry* **1995**, *34*, 5274−5287.

(52) Britt, R. D.; Zimmermann, J. L.; Sauer, K.; Klein, M. P. Ammonia Binds to the Catalytic Manganese of the Oxygen-Evolving Complex of Photosystem II. Evidence by Electron Spin-Echo Envelope Modulation Spectroscopy. *J. Am. Chem. Soc.* **1989**, *111*, 3522−3532.

(53) Schraut, J.; Kaupp, M. On Ammonia Binding to the Oxygen-Evolving Complex of Photosystem II: A Quantum Chemical Study. *Chem. - Eur. J.* **2014**, *20*, 7300−7308.

(54) Pérez Navarro, M.; Ames, W. M.; Nilsson, H.; Lohmiller, T.; Pantazis, D. A.; Rapatskiy, L.; Nowaczyk, M. M.; Neese, F.; Boussac, A.; Messinger, J.; Lubitz, W.; Cox, N. Ammonia Binding to the Oxygen-Evolving Complex of Photosystem II Identifies the Solvent-Exchangeable Oxygen Bridge (μ-oxo) of the Manganese Tetramer. *Proc. Natl. Acad. Sci. U. S. A.* **2013**, *110*, 15561−15566.

(55) Oyala, P. H.; Stich, T. A.; Debus, R. J.; Britt, R. D. Ammonia Binds to the Dangler Manganese of the Photosystem II Oxygen-Evolving Complex. *J. Am. Chem. Soc.* **2015**, *137*, 8829−8837.

(56) Askerka, M.; Vinyard, D. J.; Brudvig, G. W.; Batista, V. S. NH_3 Binding to the S_2 State of the O_2-Evolving Complex of Photosystem II: Analogue to H_2O Binding during the $S_2 \rightarrow S_3$ Transition. *Biochemistry* **2015**, *54*, 5783−5786.

(57) Vinyard, D. J.; Askerka, M.; Debus, R. J.; Batista, V. S.; Brudvig, G. W. Ammonia Binding in the Second Coordination Sphere of the Oxygen-Evolving Complex of Photosystem II. *Biochemistry* **2016**, *55*, 4432.

(58) Dismukes, G. C.; Siderer, Y. Intermediates of a Polynuclear Manganese Center Involved in Photosynthetic Oxidation of Water. *Proc. Natl. Acad. Sci. U. S. A.* **1981**, *78*, 274−278.

(59) Casey, J. L.; Sauer, K. Electron-Paramagnetic-Res. Detection of a Cryogenically Photogenerated Intermediate in Photosynthetic Oxygen Evolution. *Biochim. Biophys. Acta, Bioenerg.* **1984**, *767*, 21−28.

(60) Haddy, A.; Lakshmi, K. V.; Brudvig, G. W.; Frank, H. A. Q-band EPR of the S_2 State of Photosystem II Confirms an $S = 5/2$ Origin of the X-band $g = 4.1$ Signal. *Biophys. J.* **2004**, *87*, 2885−2896.

(61) Sproviero, E. M.; Gascon, J. A.; McEvoy, J. P.; Brudvig, G. W.; Batista, V. S. Quantum Mechanics/Molecular Mechanics Study of the Catalytic Cycle of Water Splitting in Photosystem II. *J. Am. Chem. Soc.* **2008**, *130*, 3428−3442.

(62) Capone, M.; Bovi, D.; Narzi, D.; Guidoni, L. Reorganization of Substrate Waters between the Closed and Open Cubane Conformers during the S_2 to S_3 Transition in the Oxygen Evolving Complex. *Biochemistry* **2015**, *54*, 6439−6442.

(63) Cox, N.; Retegan, M.; Neese, F.; Pantazis, D. A.; Boussac, A.; Lubitz, W. Photosynthesis. Electronic Structure of the Oxygen-Evolving Complex in Photosystem II Prior to O-O Bond Formation. *Science* **2014**, *345*, 804−808.

(64) Kupitz, C.; Basu, S.; Grotjohann, I.; Fromme, R.; Zatsepin, N. A.; Rendek, K. N.; Hunter, M. S.; Shoeman, R. L.; White, T. A.; Wang, D.; James, D.; Yang, J.-H.; Cobb, D. E.; Reeder, B.; Sierra, R. G.; Liu, H.; Barty, A.; Aquila, A. L.; Deponte, D.; Kirian, R. A.; Bari, S.; Bergkamp, J. J.; Beyerlein, K. R.; Bogan, M. J.; Caleman, C.; Chao, T.-C.; Conrad, C. E.; Davis, K. M.; Fleckenstein, H.; Galli, L.; Hau-Riege, S. P.; Kassemeyer, S.; Laksmono, H.; Liang, M.; Lomb, L.; Marchesini, S.; Martin, A. V.; Messerschmidt, M.; Milathianaki, D.; Nass, K.; Ros, A.; Roy-Chowdhury, S.; Schmidt, K.; Seibert, M.; Steinbrener, J.; Stellato, F.; Yan, L.; Yoon, C.; Moore, T. A.; Moore, A. L.; Pushkar, Y.; Williams, G. J.; Boutet, S.; Doak, R. B.; Weierstall, U.; Frank, M.; Chapman, H. N.; Spence, J. C. H.; Fromme, P. Serial Time-Resolved Crystallography of Photosystem II Using a Femtosecond X-ray Laser. *Nature* **2014**, *513*, 261−265.

(65) Siegbahn, P. E. M. Water Oxidation Mechanism in Photosystem II, Including oxidations, proton release pathways, O−O bond formation and O_2 release. *Biochim. Biophys. Acta, Bioenerg.* **2013**, *1827*, 1003−1019.

(66) Noguchi, T. FTIR Detection of Water Reactions in the Oxygen-Evolving Centre of Photosystem II. *Philos. Trans. R. Soc., B* **2008**, *363*, 1189−1194.

(67) Dau, H.; Liebisch, P.; Haumann, M. The Manganese Complex of Oxygenic Photosynthesis: Conversion of Five-Coordinated Mn(III) to Six-Coordinated Mn(IV) in the $S_2 \rightarrow S_3$ Transition is Implied by XANES Simulations. *Phys. Scr.* **2005**, *115*, 844−846.

(68) Li, X. C.; Siegbahn, P. E. M. Alternative Mechanisms for O_2 Release and O-O Bond Formation in the Oxygen Evolving Complex of Photosystem II. *Phys. Chem. Chem. Phys.* **2015**, *17*, 12168−12174.

(69) Bao, H.; Burnap, R. L. Structural Rearrangements Preceding Dioxygen Formation by the Water Oxidation Complex of Photosystem II. *Proc. Natl. Acad. Sci. U. S. A.* **2015**, *112*, E6139−6147.

(70) Vogt, L.; Vinyard, D. J.; Khan, S.; Brudvig, G. W. Oxygen-Evolving Complex of Photosystem II: an Analysis of Second-Shell Residues and Hydrogen-Bonding Networks. *Curr. Opin. Chem. Biol.* **2015**, *25*, 152−158.

(71) Retegan, M.; Krewald, V.; Mamedov, F.; Neese, F.; Lubitz, W.; Cox, N.; Pantazis, D. A. A Five-Coordinate Mn (IV) Intermediate in Biological Water Oxidation: Spectroscopic Signature and a Pivot Mechanism for Water Binding. *Chem. Sci.* **2016**, *7*, 72−84.

(72) Capone, M.; Narzi, D.; Bovi, D.; Guidoni, L. Mechanism of Water Delivery to the Active Site of Photosystem II Along the S_2 to S_3 Transition. *J. Phys. Chem. Lett.* **2016**, *7*, 592−596.

(73) Vassiliev, S.; Zaraiskaya, T.; Bruce, D. Exploring the Energetics of Water Permeation in Photosystem II by Multiple Steered Molecular Dynamics Simulations. *Biochim. Biophys. Acta, Bioenerg.* **2012**, *1817*, 1671−1678.